Contribution from the Chemistry Department,
Brookhaven National Laboratory, Upton, New York 11973

Donor-Acceptor Electronic Coupling as a Function of Bridging Group: Mixed-Valence Diruthenium(II,III) Complexes Bridged by Isonicotinato and Isonicotinamido Ligands

Mei H. Chou, Carol Creutz,* and Norman Sutin*

Received January 9, 1992

Binuclear, mixed-valence μ-isonicotinato and μ-isonicotinamido complexes capped by pentaammineruthenium(II) at the pyridine site and pentaammineruthenium(III) at the carboxylato or amido site have been synthesized and characterized. On the basis of their electronic absorption spectra and redox properties, the amido complexes are assigned as the N-bonded (Ru^{III}-NHC(O)R) isomers. The mixed-valence complexes exhibit intervalence charge-transfer bands at 720 nm ($\epsilon = 2.6 \times 10^2$ M^{-1} cm^{-1}) and 761 nm (0.9×10^3 M^{-1} cm^{-1}), respectively, in aqueous acetate buffer at pH 4.8. The redox potentials of the two sites differ by 0.44 V in the isonicotinato and by 0.54 V in the isonicotinamido complexes in the above medium, and the donor-acceptor coupling elements, evaluated from the intensities of the intervalence bands, are 300 and 510 cm^{-1}, respectively. Solvent dependences of the electronic spectra and electrochemical parameters are also reported. Both bridges provide significant coupling between the Ru(II) and Ru(III) metal centers in the mixed-valence complexes. These coupling energies serve as a point of departure for a consideration of coupling mechanisms in related polyproline-bridged systems for which thermal electron-transfer rates have been determined. It is concluded that "hole" transfer pathways predominate when osmium(II) pentaammine is the donor and cobalt(III) or ruthenium(III) pentaammine is the electron acceptor.

Introduction

The physical properties of mixed-valence complexes[1] have been widely used as a probe of the donor-acceptor interactions that are of fundamental interest in the electron-transfer field.[1,2] In systems of moderate donor-acceptor electronic coupling, the positions and intensities of donor-acceptor (metal-to-metal or intervalence) charge-transfer bands yield information about the energetic barriers to electron transfer and the magnitude of the donor-acceptor electronic coupling element, respectively.[3] Probably the largest body of MMCT data is that for bridged pentaammineruthenium complexes $(NH_3)_5Ru^{II}(bridge)Ru^{III}(NH_3)_5$. The bridges investigated range from symmetric ligands such as 4,4'-bipyridine[4] to asymmetric bridging groups such as 4-cyanopyridine.[5] In the present report, we describe the syntheses and properties of two new asymmetric mixed-valence species, one bridged by an isonicotinato

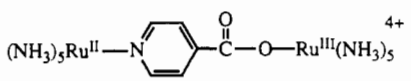

and the other, by an isonicotinamido (the singly deprotonated isonicotinamide) ligand.

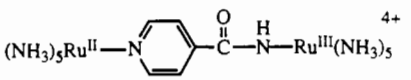

These new species are of interest in their own right and in the context of electron transfer in polypeptide-bridged species. Isied and colleagues[6] have reported the dependence of the electron-transfer rates in polyproline-bridged osmium(II)-ruthenium(III) species

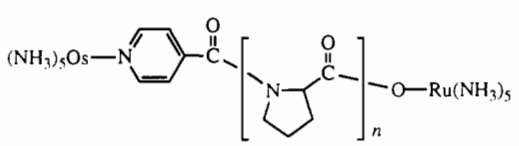

on the number of proline groups n, for which the $n = 0$ derivative is the isonicotinato-bridged complex. Because of our interest in the electronic properties of the isonicotinate bridge, we decided to examine the diruthenium analog and the isoelectronic μ-amido complex.

Experimental Section

Isonicotinic acid, isonicotinamide, 4-cyanopyridine, and ammonium hexafluorophosphate were used as obtained from Aldrich. Trifluoromethanesulfonic (triflic) acid was purchased from Alfa, and hexaammineruthenium(III) trichloride, from Mathey-Bishop, Inc.

$Ru(NH_3)_5(H_2O)(CF_3SO_3)_3$. Aquopentaammineruthenium(III) triflate was prepared by hydrolysis of chloropentaammineruthenium(III) which had been prepared from the hexaammine complex.[7] To 1 g of $Ru(NH_3)_5Cl(Cl)_2$ in 50 mL of water was added 6 mL of deaerated 58% NH_4OH, and the mixture was stirred under argon for 1 h. A 10-mL aliquot of saturated aqueous $Na_2S_2O_6$ was added, and the solution was stirred for another 2 h and then cooled in an ice bath. The pale yellow $Ru(NH_3)_5(OH)(S_2O_6)$ which formed was collected on a filter (0.78 g, 62%). The solid was added to 10 mL of 2.3 M triflic acid, heated at 50 °C for 15 min, and then filtered. The desired solid formed when 1 mL of concentrated triflic acid was added to the filtrate, and the resulting solution was cooled in an ice bath.

$Ru(NH_3)_5(isonicotinic\ acid)(PF_6)_2$. $Ru(NH_3)_5(H_2O)(CF_3SO_3)_3$ (0.3 g) was dissolved in 4.5 mL of 10^{-3} M triflic acid and bubbled with argon for 50 min. Amalgamated zinc was added, and the solution was bubbled further for 40 min and then transferred by syringe to another deaerated serum bottle containing 0.1 g of isonicotinic acid. The solution was stirred for 45 min and then filtered; 1 mL of 1.25 M triflic acid and 1 g of NH_4PF_6 were added to the filtrate, which was then cooled in an ice bath. The very fine precipitate which resulted was collected on a filter and washed with diethyl ether. $Ru(NH_3)_5(isonicotinamide)(PF_6)_2$ was prepared by the same method.

$[Ru(NH_3)_5(\mu\text{-isonicotinato})Ru(NH_3)_5](PF_6)_4$. $Ru(NH_3)_5(H_2O)(CF_3SO_3)_3$ (0.15 g) was dissolved in 2.3 mL of water, and the solution was bubbled with argon for 30 min. Amalgamated zinc was added, and the solution was bubbled further for 40 min and then transferred by syringe to another deaerated serum bottle containing 28.5 mg of isonicotinic acid. The solution was stirred in the dark for 1 h. Solid $Ru(NH_3)_5(H_2O)(CF_3SO_3)_3$ (0.15 g) and a solution of 15 mg of $Ru(NH_3)_5(H_2O)(CF_3SO_3)_3$ in 0.5 mL of water, reduced over amalgamated zinc, were then added to the red solution of the mononuclear isonicotinate complex. Under argon the pH of the mixture was adjusted to 3.45 with 0.1 M aqueous $NaHCO_3$ and the solution was stirred in the dark for 1.5 h. The solution was then opened to the air and filtered, and 1 g of NH_4PF_6 was added to the filtrate. The product was collected on a filter, washed three times with 5 mL of diethyl ether, and dried in a vacuum dessicator. Yield: 0.2 g (80%). Chromatography on SP Sephadex C-25 indicated that the binuclear species (which was readily eluted by 0.7 M NaCl) was contaminated by only a small amount (<3%) of the mononuclear isonicotinate (which was eluted by 0.2 M NaCl). The diruthenium(III) complex was not isolated as a solid but was generated by persulfate oxidation of the 4+ ion in situ.

Isonicotinamido-Bridged Complexes. Two synthetic strategies were tried: The first involved direct assembly (with Ru(II) catalysis) as proved successful for the carboxylate. Since the maximum formation of the binuclear complex was only about 50% under the conditions used, the product had to be purified by cation-exchange chromatography. The

(1) Creutz, C. *Prog. Inorg. Chem.* **1983**, *30*, 1-73.
(2) Sutin, N. *Prog. Inorg. Chem.* **1983**, *30*, 441-498.
(3) Hush, N. S. *Prog. Inorg. Chem.* **1967**, *8*, 391-444.
(4) Sutton, J. E.; Sutton, P. M.; Taube, H. *Inorg. Chem.* **1979**, *18*, 1017-1021.
(5) Richardson, D. E.; Taube, H. *J. Am. Chem. Soc.* **1983**, *105*, 40-51.
(6) Vassilian, A.; Wishart, J. F.; van Hemelryck, B.; Schwarz, H.; Isied, S. S. *J. Am. Chem. Soc.* **1990**, *112*, 7278-7286.
(7) Vogt, L. H.; Katz, L.; Wiberley, S. E. *Inorg. Chem.* **1965**, *4*, 1157-1163.

0020-1669/92/1331-2318$03.00/0

other strategy, which gave the diruthenium(III) complex $[Ru(NH_3)_5(\mu\text{-isonicotinamido})Ru(NH_3)_5](PF_6)_5$, involved oxidation of the binuclear 4-cyanopyridine complex. In the Ru(III)–Ru(III) state, the latter rapidly undergoes hydrolysis to the amide.

$[Ru(NH_3)_5(\mu\text{-isonicotinamido})Ru(NH_3)_5](PF_6)_4$. The procedure given above for the isonicotinate dimer was followed; preparations run at pH 5, 7 and 8 gave the same yield (about 50%) of the binuclear species, as assessed by cation-exchange chromatography and by the relative currents of the peaks in the differential pulse voltammograms. In one instance a small amount of relatively pure triflate salt separated prior to the addition of ammonium hexafluorophosphate. A small sample of purified hexafluorophosphate salt was prepared by preparative-scale cation-exchange chromatography: 100 mg of the crude solid was dissolved in 20 mL of 0.01 M triflic acid, and the solution was loaded onto 6 mL of Sephadex C-25 (0.2-cm-diameter column). The mononuclear complex $Ru(NH_3)_5(isonicotinamide)^{2+}$ was eluted by 0.2 M lithium triflate; the binuclear complex was eluted with 0.4 and 0.5 M lithium triflate. A solid (16 mg) was obtained when 2 g of NH_4PF_6 was added to the ca. 100 mL of the latter eluant after it had been reduced to 50 mL on a rotary evaporator.

$[Ru(NH_3)_5(\mu\text{-isonicotinamido})Ru(NH_3)_5](PF_6)_5$. To the binuclear 4-cyanopyridine complex[5] $[Ru(NH_3)_5(\mu\text{-4-cyanopyridine})Ru(NH_3)_5](PF_6)_4$ (0.078 g) and 1 equiv (20.2 mg) of $K_2S_2O_8$ was added 6 mL of millimolar triflic acid. The mixture was stirred until a yellow solution was obtained. The solution was filtered, and NH_4PF_6 was added after 1 h. The solid hexafluorophosphate salt which formed was collected on a filter and washed with a few drops of water and then with diethyl ether. UV–vis in 1 mM triflic acid, λ_{max}, nm (ϵ, M^{-1} cm^{-1}): 348 (5.2×10^3), 272 (5.7×10^3).

UV–vis spectra were determined with Cary 210 or Hewlett-Packard 8452A diode array spectrometers; the near-IR region was investigated with use of an Olis adapted Cary 14 instrument. Electrochemical experiments (cyclic voltammetry and differential pulse voltammetry) were carried out with a BAS electrochemical analyzer, with a glassy-carbon working electrode, platinum-wire auxiliary electrode, and saturated calomel (SCE) reference electrode in a conventional H cell. The rate of nitrile hydrolysis of the fully oxidized cyanopyridine complex was determined with a HiTech SFA-11/1025 hand-driven stopped-flow instrument with its sample cell positioned in a Hewlett-Packard 8452A diode array spectrometer. Data were collected at ca. 1-s intervals in the wavelength range 220–500 nm.

Results

Mononuclear Complexes. Despite the fact that complexes of pentaammineruthenium(II) and -(III) with aromatic N-heterocycles,[8] nitriles,[9-11] carboxylates,[12,13] and amides[11,14-18] have received rather extensive attention in the past, we found it necessary to characterize selective aspects of the properties of the mononuclear complexes in order to prepare and understand the properties of the binuclear species which are the emphasis of this paper. Those of the mononuclear amido complexes are reported separately.[19]

The pK_a of the pentaammineruthenium(II) isonicotinic acid complex (important in the synthesis of the binuclear complex) was first crudely estimated to be 3.45 from the pH (3.36) of a millimolar solution of the complex in water. A more systematic study of the pH dependence of the visible spectrum of the ruthenium(II) complex in 0.1 M triflate medium gave pK_a 3.0 at 25 °C. From the dependence of the Ru(III)/(II) reduction potential on pH in 0.1 M triflate at 22 ± 2 °C, pK_a values of 3.0 ± 0.2 and 2.0 ± 0.2 were obtained for the ruthenium(II) and -(III) complexes, respectively.

Table I. Properties of Free Ligands and Mononuclear Pentaammineruthenium Complexes[a]

	4-pyC(O)OH	4-pyC(O)O⁻	4-pyC(O)NH₂
$E°(Ru^{III/II})$, V vs NHE	+0.382[d] +0.395	+0.34	+0.44[c] +0.375[d]
$pK(Ru^{II})$	3.0 ± 0.2		
$pK(Ru^{III})$	2.0 ± 0.2		
	Complex		
λ_{max}, nm	497[b]	457[b]	479[b]
(ϵ, M^{-1} cm^{-1})	492 (1.0×10^4)[g] 264 (3.7×10^3)[g]	460 (9.6×10^3)[f] 256 (1.6×10^3)[f]	478 (1.1×10^4)[c] 260 (3.7×10^3)[c]
	Free Ligand		
λ_{max}, nm	270 (4.1×10^3)[g]	262 (2.5×10^3)[e]	268 (2.6×10^3)[e]
(ϵ, M^{-1} cm^{-1})	216 (5.9×10^3)[g]	202 (8.0×10^3)[e]	204 (7.6×10^3)[e]

[a] Data from this study in 0.1 M KCF_3SO_3 unless otherwise noted. [b] Ru(II) complex. Ford, P.; Rudd, D. F. P.; Gaunder, R.; Taube, H. *J. Am. Chem. Soc.* **1968**, *90*, 1187–1194. [c] Gaunder, R. G.; Taube, H. *Inorg. Chem.* **1970**, *9*, 2627. Spectrum in 0.1 M $HClO_4$; $E°$ determined in 1.0 M chloride medium. [d] Matsubara, T.; Ford, P. C. *Inorg. Chem.* **1976**, *15*, 1107. 0.1 M *p*-toluenesulfonic acid/0.1 M potassium *p*-toluenesulfonate medium. [e] In pH 8, 0.02 M phosphate buffer. [f] In aqueous pH 6.8 phosphate buffer. [g] In 0.1 M triflic acid.

Since comparable data for the pentaammineruthenium isonicotinamide complexes would be useful in understanding the thermodynamics of their formation, we also examined the pH dependence of the oxidation of this ruthenium(II) complex in a 1 M potassium triflate medium. In 0.02 M buffer solutions at pH 5 (acetate), 8 (acetate), and 9.3 (carbonate), the Ru(III)/(II) couple was chemically reversible with a potential of (+0.40 ± 0.01) V vs NHE; in pH 10.8 carbonate buffer and in more alkaline solutions (0.01, 0.1, and 0.5 M NaOH), only the anodic portion of the CV was observed and the potential shifted to more negative values with a slope of ca. 59 mV/pH unit. This behavior is suggestive of a pK near pH 10.5, probably due to deprotonation of an ammine ligand on the Ru(III) complex; the chemical irreversibility is probably due to disproportionation of the ruthenium(III) complex.[20]

The UV spectra of the free ligands were determined as an aid to the interpretation of the dimer spectra. These results, as well as our other spectral and electrochemical results for mononuclear species, are summarized in Table I.

Binuclear Complexes. L = μ-Isonicotinate. In a series of preliminary experiments, the kinetics and yield of the formation of the bridged complex from 1×10^{-3} M $(NH_3)_5Ru(4\text{-}pyCO_2)^+$ and 40×10^{-3} M $(NH_3)_5RuOH_2^{3+}$ (eq 1), catalyzed by 4×10^{-3}

$$(NH_3)_5Ru(4\text{-}pyCO_2)^+ + (NH_3)_5RuOH_2^{3+} \rightleftharpoons (NH_3)_5Ru(4\text{-}pyCO_2)Ru(NH_3)_5^{4+} + H_2O \quad (1)$$

M $(NH_3)_5RuOH_2^{2+}$, were followed at 720 nm in a 1-cm cell and at 470 nm in a 2-mm cell. The growth of the product absorbance was exponential, with a pseudo-first-order rate constant k_{obs} of 0.6×10^{-3} s^{-1} at pH 3.5 and 0.3×10^{-3} s^{-1} at pH 2.6. The yields obtained (based on the molar absorptivities of the purified dimer) are consistent with a binding constant for eq 1 of ca. 10^4 M^{-1} at 22 ± 2 °C. The preparative-scale work was carried out at pH 3.5 to minimize deprotonation of $(NH_3)_5RuOH_2^{3+}$ (eq 2, pK ca. 4) and maximize the concentration of $(NH_3)_5Ru(4\text{-}pyCO_2)^+$ (eq 3, pK 3).

$$(NH_3)_5RuOH_2^{3+} \rightleftharpoons (NH_3)_5RuOH^{2+} + H^+ \quad (2)$$

$$(NH_3)_5Ru(4\text{-}pyCO_2H)^{2+} \rightleftharpoons (NH_3)_5Ru(4\text{-}pyCO_2)^+ + H^+ \quad (3)$$

L = μ-Isonicotinamido. Direct Assembly of the Mixed-Valence Complex. The direct approach (eq 4 below pH 4) produced small absorbance increases in the 720–760-nm region at pH 1–3, and

$$(NH_3)_5Ru(4\text{-}pyC(O)NH_2)^{2+} + (NH_3)_5RuOH_2^{3+} \rightleftharpoons (NH_3)_5Ru(4\text{-}pyC(O)NH)Ru(NH_3)_5^{4+} + H_3O^+ \quad (4)$$

these increased in magnitude with pH. With 1×10^{-3} M

(8) Ford, P.; Rudd, D. F. P.; Gaunder, R.; Taube, H. *J. Am. Chem. Soc.* **1968**, *90*, 1187–1194.
(9) Clarke, R. E.; Ford, P. C. *Inorg. Chem.* **1970**, *9*, 227–235.
(10) Clarke, R. E.; Ford, P. C. *Inorg. Chem.* **1970**, *9*, 495–499.
(11) Zanella, A. W.; Ford, P. C. *Inorg. Chem.* **1975**, *14*, 42–47.
(12) Stritar, J. A.; Taube, H. *Inorg. Chem.* **1969**, *8*, 2281–2292.
(13) Ohyoshi, A.; Yoshikuni, K. *Bull. Chem. Soc. Jpn.* **1979**, *52*, 3105–3106.
(14) Diamond, S. E.; Taube, H. *J. Chem. Soc., Chem. Commun.* **1974**, 622–623.
(15) Diamond, S. E.; Grant, B.; Tom, G. M.; Taube, H. *Tetrahedron Lett.* **1974**, 4025–4028.
(16) Ilan, Y.; Taube, H. *Inorg. Chem.* **1983**, *22*, 1655–1664.
(17) Huang, H.-Y.; Chen, W.-J.; Yang, C.-C.; Yeh, A. *Inorg. Chem.* **1991**, *30*, 1862–1868.
(18) Fairlie, D. P.; Taube, H. *Inorg. Chem.* **1985**, *24*, 3199–3206.
(19) Chou, M. H.; Szalda, D. J.; Creutz, C.; Sutin, N. *Inorg. Chem.*, to be submitted for publication.
(20) Rudd, D. P.; Taube, H. *Inorg. Chem.* **1971**, *10*, 1543–1544.

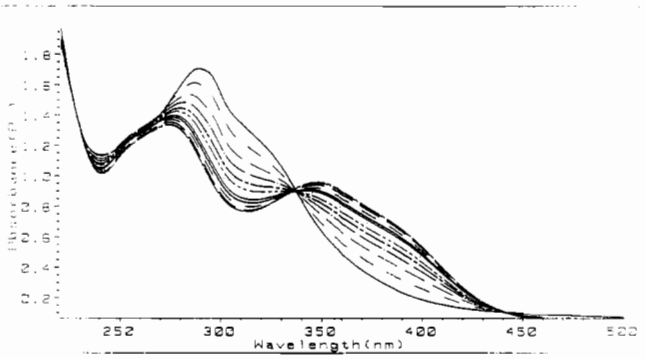

Figure 1. Hydrolysis of $(NH_3)_5Ru(4\text{-}pyCN)Ru(NH_3)_5^{6+}$ (λ_{max} 288 nm) to $(NH_3)_5Ru(4\text{-}pyC(O)NH)Ru(NH_3)_5^{5+}$ (λ_{max} 355, 274 nm) at 25 °C in 0.1 M KCF_3SO_3 containing 10^{-3} M acid.

$(NH_3)_5Ru(4\text{-}pyC(O)NH_2)^{2+}$, 40×10^{-3} M $(NH_3)_5RuOH_2^{3+}$, and 4×10^{-3} M $(NH_3)_5RuOH_2^{2+}$ catalyst, the growth of the absorbance at 750 nm was exponential with a pseudo-first-order rate constant k_{obs} of 0.4×10^{-3} s^{-1} at pH 3.8, 0.1×10^{-3} s^{-1} at pH 4.8, and 0.5×10^{-3} s^{-1} at pH 8.7. In an effort to favor the binding thermodynamics, which become more favorable at higher pH because of eq 5 ($pK \geq 10.5$), the reaction was run at higher pH

$$(NH_3)_5Ru(4\text{-}pyC(O)NH_2)^{2+} \rightleftharpoons (NH_3)_5Ru(4\text{-}pyC(O)NH)^{+} + H^{+} \quad (5)$$

as well. The yields (based on the molar absorptivities of the column-purified dimer), based on eq 6, were the same at pH 4.8, 6.8, and 8.7, consistent with eq 6 and an equilibrium quotient of $K_6 = 6.5 \pm 1$ M^{-1} at 22 ± 2 °C.

$$(NH_3)_5Ru(4\text{-}pyC(O)NH_2)^{2+} + (NH_3)_5RuOH^{2+} \rightleftharpoons (NH_3)_5Ru(4\text{-}pyC(O)NH)Ru(NH_3)_5^{4+} + H_2O \quad (6)$$

Purified (chromatographed) samples of $(NH_3)_5Ru(4\text{-}pyC(O)NH)Ru(NH_3)_5^{4+}$ had essentially the same absorption spectra as samples prepared by hydrolysis of the μ-4-cyanopyridine complex, followed by reduction with hexaammineruthenium(II) (vide infra). However, in some samples the intensity of the ca. 500–510-nm shoulder was greater and solutions prepared from aged solids exhibited increased absorption at 340–350 nm. We attribute these absorptions to contamination (<5%) by ruthenium red ($\epsilon_{532} = 7 \times 10^4$ M^{-1} cm^{-1}) or its oxidation product ruthenium brown ($\epsilon_{350} = 1.4 \times 10^4$ M^{-1} cm^{-1})[21] or to related oxy-bridged polynuclear species. The formation of ruthenium red is promoted in basic, concentrated solutions of $Ru(NH_3)_5OH^{2+}$, especially in the presence of carbonate. Ruthenium brown, the one-electron oxidation product of ruthenium red, forms upon air oxidation of ruthenium red in acid.

Preparation via Hydrolysis of the Diruthenium(III) μ-4-Cyanopyridine Complex. Although $(NH_3)_5Ru(4\text{-}pyCN)Ru(NH_3)_5^{6+}$ is sufficiently stable in water at pH 3 to be observed in cyclic voltammograms of $(NH_3)_5Ru(4\text{-}pyCN)Ru(NH_3)_5^{4+}$ run at moderate scan rates, oxidation of the (millimolar) Ru(II) dimer by 2 equiv of Ce(IV) or peroxydisulfate yields the cyclic voltammogram of the isonicotinamido species in less than 1 min. The hydrolysis of the oxidized cyanopyridine complex (eq 7) was

$$(NH_3)_5Ru(4\text{-}pyCN)Ru(NH_3)_5^{6+} + H_2O \rightarrow (NH_3)_5Ru(4\text{-}pyC(O)NH)Ru(NH_3)_5^{5+} + H^{+} \quad (7)$$

monitored by stopped-flow spectrophotometry: 2×10^{-3} M $(NH_3)_5Ru(4\text{-}pyCN)Ru(NH_3)_5^{4+}$ and 20×10^{-3} M $K_2S_2O_8$ (known to rapidly oxidize ruthenium(II) complexes of this type[22,23]) were mixed by a hand-driven Hi-Tech stopped-flow instrument and collected in the cell compartment of a diode array spectrophotometer where the spectra were monitored for several minutes. The initial spectrum ($(NH_3)_5Ru(4\text{-}pyCN)Ru(NH_3)_5^{6+}$), with maxima at 288 nm ($\epsilon = 0.85 \times 10^3$ M^{-1} cm^{-1}) and 320 nm (shoulder, $\epsilon = 0.6 \times 10^3$ M^{-1} cm^{-1}), evolved exponentially to that of the μ-amido complex (maxima at 355 nm ($\epsilon = 0.5 \times 10^4$ M^{-1} cm^{-1}) and 274 nm ($\epsilon = 0.64 \times 10^4$ M^{-1} cm^{-1}) with a rate constant of 0.025 s^{-1} at 25.0 °C. The results are shown in Figure 1. The oxidation-induced hydrolysis eq 7 was used on a preparative scale to prepare the samples that were used to determine the solvent dependence of the reduction potentials.

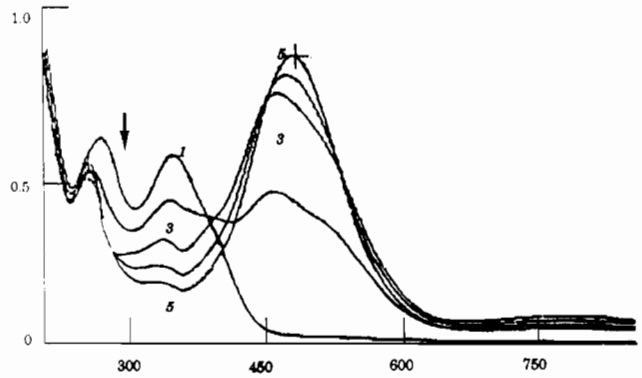

Figure 2. UV–vis spectra (*x*-axis in nanometers) obtained upon reduction with $Ru(NH_3)_6^{2+}$ of $(NH_3)_5Ru(4\text{-}pyC(O)NH)Ru(NH_3)_5^{5+}$ prepared by the hydrolysis of the 4-cyanopyridine dimer.

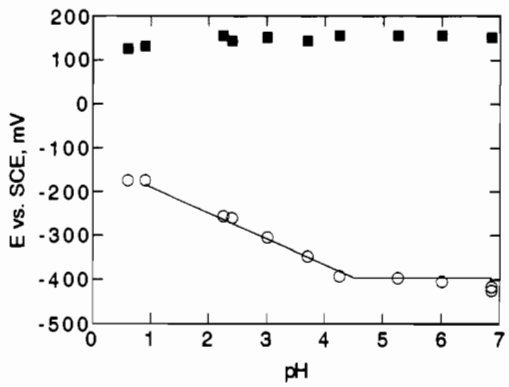

Figure 3. pH dependence of reduction potentials for $(NH_3)_5Ru(4\text{-}pyC(O)NH)Ru(NH_3)_5^{n+}$ species in 0.5 M potassium triflate at 22 ± 2 °C. The solid lines are imposed for the pK_a and $E_{1/2}$ values summarized in Scheme I.

As is shown in Figure 2, treatment of $(NH_3)_5Ru(4\text{-}pyC(O)NH)Ru(NH_3)_5^{5+}$, prepared by eq 7, with 1 equiv of $Ru(NH_3)_6^{2+}$ yielded $(NH_3)_5Ru(4\text{-}pyC(O)NH)Ru(NH_3)_5^{4+}$ (eq 8). When more $Ru(NH_3)_6^{2+}$ was added, hydrolysis of the resulting diruthenium(II) complex to the mononuclear isonicotinamide complex occurred.

$$(NH_3)_5Ru(4\text{-}pyC(O)NH)Ru(NH_3)_5^{5+} + Ru(NH_3)_6^{2+} \rightarrow (NH_3)_5Ru(4\text{-}pyC(O)NH)Ru(NH_3)_5^{4+} + Ru(NH_3)_6^{3+} \quad (8)$$

pH Dependences. The electrochemical and spectral properties of the isonicotinato-bridged complexes were pH-independent in the region we investigated, giving the following pK_a limits: $(NH_3)_5Ru(4\text{-}pyCO_2H)Ru(NH_3)_5^{6+}$, ≤−0.7; $(NH_3)_5Ru(4\text{-}pyCO_2H)Ru(NH_3)_5^{5+}$ and $(NH_3)_5Ru(4\text{-}pyCO_2H)Ru(NH_3)_5^{4+}$, ≤0.

Differential pulse voltammograms of $(NH_3)_5Ru(4\text{-}pyC(O)NH)Ru(NH_3)_5^{5+}$ and $(NH_3)_5Ru(4\text{-}pyC(O)NH)Ru(NH_3)_5^{4+}$ were carried out as a function of pH in a 0.5 M KCF_3SO_3 medium in order to determine the pK_a and $E_{1/2}$ values of the various species. The results are shown in Figure 3. The pK_a of $(NH_3)_5Ru(4\text{-}pyC(O)HNH)Ru(NH_3)_5^{6+}$ is estimated as −0.6 from the $[H^+]$ dependence of the UV–vis spectrum: The intensity of the 347-nm band diminishes with increasing triflic acid concentration in the 2–4 M range. In 6 M acid the band is effectively bleached and the 280-nm band has increased ca. 50% in intensity, developing

(21) Earley, J. E.; Fealey, T. *Inorg. Chem.* **1973**, *12*, 323–327.
(22) Fürholz, U.; Haim, A. *Inorg. Chem.* **1987**, *26*, 3243–3248.
(23) Olabe, J. A.; Haim, A. *Inorg. Chem.* **1989**, *28*, 3277–3278.

Table II. Ruthenium(III)/(II) Reduction Potentials of the Binuclear μ-L Complexes vs the Ferrocenium/Ferrocene Couple as a Function of Solvent at 22 ± 2 °C in 0.1 M Tetrabutylammonium Hexafluorophosphate (Organic Solvents) or 0.1 M Potassium Triflate (Water)

	solvent (donor no.)				
	CH_3NO_2 (2.7)	CH_3CN (14.1)	H_2O (18)	$HC(O)N(CH_3)_2$ (26.6)	$(CH_3)_2SO$ (29.8)
			L = Isonicotinato[a]		
$E_{1/2}$(py), V	0.39	0.076	0.025	−0.32	−0.36
$E_{1/2}(CO_2)$, V	−0.26	−0.56	−0.41	−0.86	−0.90
ΔE, V	0.67	0.60	0.44	0.54	0.54
			L = Isonicotinamido[b]		
$E_{1/2}$(py), V	c	0.084	0.023	−0.27	−0.35
$E_{1/2}$(C(O)NH), V		−0.68	−0.52	−1.00	−1.05
ΔE, V		0.76	0.54	0.71	0.71

[a] Obtained with the PF_6^- salt of the Ru(II)/Ru(III) complex. [b] Obtained with the PF_6^- salt of the Ru(III)/Ru(III) complex. [c] Neither the $CF_3SO_3^-$ nor the PF_6^- salt was soluble in nitromethane.

Table III. Solvent Dependence of the Electronic Absorption Spectra of Mixed-Valence $((NH_3)_5Ru)_2L$ Complexes

	solvent (donor no.)			
	CH_3NO_2 (2.7)	CH_3CN (14.1)	$HC(O)N(CH_3)_2$ (26.6)	$(CH_3)_2SO$ (29.8)
		L = μ-Isonicotinato		
λ_{max}, nm (ϵ, M^{-1} cm^{-1})	728 (299)[a]	724 (303)[a]	748 (316)[a]	776 (274)[a]
	718 (317)[b]	720 (277)[b]	754 (279)[b]	770 (203)[b]
	460 (6.7 × 10^3)	466 (6.4 × 10^3)	496 (7.5 × 10^3)	500 (6.7 × 10^3)
		300 (sh) (1.8 × 10^3)	300 (sh) (2.0 × 10^3)	300 (sh) (2.0 × 10^3)
		260 (3.9 × 10^3)		
		L = μ-Isonicotinamido		
λ_{max}, nm (ϵ, M^{-1} cm^{-1})	726 (1.2 × 10^3)[b]	734 (1.3 × 10^3)	796 (1.3 × 10^3)	818 (1.1 × 10^3)
	500 (sh) (8.5 × 10^3)	502 (sh) (8.2 × 10^3)	520 (sh) (1.0 × 10^4)	520 (sh) (8.5 × 10^3)
	458 (9.6 × 10^3)	448 (1.0 × 10^4)	486 (1.0 × 10^4)	480 (8.5 × 10^3)
		348 (3.7 × 10^3)	350 (4.7 × 10^3)	358 (3.3 × 10^3)
		250 (4.7 × 10^3)		

[a] No added electrolyte. [b] In the presence of 0.1 M tetrabutylammonium hexafluorophosphate.

a shoulder at ca. 310 nm. The same spectrum is observed within 30 s of mixing and after 1 h. Dilution of the 6 M solution to 2 and 4 M acid yields the same spectra as are obtained when the diruthenium(III) complex is added directly to acid at these concentrations. The pK_a of $(NH_3)_5Ru(4\text{-}pyC(OH)NH)Ru(NH_3)_5^{5+}$ was estimated as 0.6 from the electrochemical experiments, but this value could not be reproduced in UV–vis experiments. In the latter, decomposition of the sample took place at a rate that increased with acid concentration, but no systematic evidence for a pK_a of 0.6 was found. Thus 0.6 is an upper limit on the pK_a of $(NH_3)_5Ru(4\text{-}pyC(OH)NH)Ru(NH_3)_5^{5+}$; accordingly, the value $E_{am,H}$ = 0.07 V is a lower limit for the $(NH_3)_5Ru(4\text{-}pyC(OH)NH)Ru(NH_3)_5^{5+/4+}$ couple. The pK_a and $E_{1/2}$ values inferred for this system are summarized in Scheme I where A = NH_3.

The reduction potentials and electronic absorption spectra of the binuclear comples were determined as a function of solvent. These results are presented in Tables II and III.

Scheme I

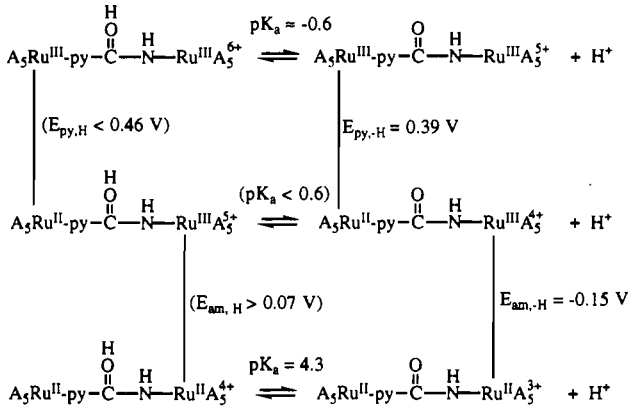

Discussion

Syntheses. As one route to the μ-amido complexes, we used the hydrolysis of the diruthenium(III) μ-4-cyanopyridine complex. Nitrile hydrolysis has been exploited fairly broadly as an entry to the amido complexes[11,14,15,17,24] and warrants little comment here. We note, however, the relative rapidity of the present system. The hydrolysis rate constant, 0.025 s^{-1} at 25 °C, is more rapid than that for all other Ru(III) complexes[11,17,34] studied except that of 4-$NCpyCH_3^+$ (k = 0.028 s^{-1}),[17] the N-pyridine-methylated derivative of 4-cyanopyridine. Since the rapidity of the hydrolysis was not appreciated in earlier work, the literature spectrum reported for $(NH_3)_5Ru^{III}(4\text{-}NCpy)Ru^{III}(NH_3)_5^{6+}$ is actually that of the μ-amido complex;[5] the spectrum of the μ-4-cyanopyridine complex is shown in Figure 1.

The chief preparative technique used here, and first exploited by Stritar and Taube,[12] involves the relatively straightforward strategy of combining the "ligand" $(NH_3)_5Ru(4\text{-}pyR)^+$, where R = CO_2^- or $C(O)NH_2$, with $(NH_3)_5RuOH_2^{3+}$ in the presence of the catalyst $(NH_3)_5RuOH_2^{2+}$. The catalysis involves both substitutional (eq 9) and electron-transfer (eq 10) steps. When

(24) Fairlie, D. P.; Angus, P. M.; Fenn, M. D.; Jackson, W. G. *Inorg. Chem.* **1991**, *30*, 1564–1569.
(25) Isied, S. S.; Vassilian, A.; Wishart, J. F.; Creutz, C.; Schwarz, H. A.; Sutin, N. *J. Am. Chem. Soc.* **1988**, *110*, 635–637.
(26) Stanbury, D. M.; Haas, O.; Taube, H. *Inorg. Chem.* **1980**, *19*, 518–524.
(27) Ohyoshi, A.; Shida, S.; Izuchi, S.; Kitigawa, F.; Ohkubo, K. *Bull. Chem. Soc. Jpn.* **1973**, *46*, 2431–2434.
(28) Lim, H. S.; Barclay, D. J.; Anson, F. C. *Inorg. Chem.* **1972**, *11*, 1460–1466.
(29) Shepherd, R.; Taube, H. *Inorg. Chem.* **1973**, *12*, 1392–1401.
(30) Yeh, A.; Taube, H. *Inorg. Chem.* **1980**, *19*, 3740–3742.
(31) Taube, H. *Comments Inorg. Chem.* **1981**, *1*, 17–31.
(32) Sigel, H.; Martin, R. B. *Chem. Rev.* **1982**, *82*, 385–426.
(33) Matsubara, T.; Ford, P. C. *Inorg. Chem.* **1976**, *15*, 1107–1110.
(34) Schäffer, L. J.; Taube, H. *J. Phys. Chem.* **1986**, *90*, 3669–3673.

$$(NH_3)_5Ru^{II}(4\text{-pyR}) + (NH_3)_5RuOH_2^{2+} \rightleftharpoons (NH_3)_5Ru^{II}(4\text{-pyR})Ru^{II}(NH_3)_5 + H_2O \quad (9)$$

$$(NH_3)_5Ru^{II}(4\text{-pyR})Ru^{II}(NH_3)_5 + (NH_3)_5RuOH_2^{3+} \rightleftharpoons (NH_3)_5Ru^{II}(4\text{-pyR})Ru^{III}(NH_3)_5 + (NH_3)_5RuOH_2^{2+} \quad (10)$$

the system has reached equilibrium, the catalyst is quenched by reaction with oxygen. (Attempts to use CH_3CN as quenching agent[25] resulted in decomposition of the binuclear complex to $(NH_3)_5Ru^{III}(4\text{-pyR})$ and $(NH_3)_5Ru(CH_3CN)^{2+}$.) The "quenching" step is imperative, because workup can result in dissociation of the complex if the Ru(II) catalyst remains present. However, the solutions cannot be left long in the presence of air, because O_2 slowly oxidizes the Ru^{II}py moiety as well.[26] An additional potential complication for the bridged mixed-valence complexes of isonicotinate and isonicotinamide is eqs 11–13 which

$$(NH_3)_5Ru^{II}(4\text{-pyR})Ru^{III}(NH_3)_5 \rightleftharpoons (NH_3)_5Ru^{III}(4\text{-pyR})Ru^{II}(NH_3)_5 \quad (11)$$

$$(NH_3)_5Ru^{III}(4\text{-pyR})Ru^{II}(NH_3)_5 \rightleftharpoons (NH_3)_5Ru^{III}(4\text{-pyR}) + (NH_3)_5RuOH_2^{2+} \quad (12)$$

$$(NH_3)_5Ru^{III}(4\text{-pyR}) + (NH_3)_5RuOH_2^{2+} \rightleftharpoons (NH_3)_5Ru^{II}(4\text{-pyR}) + (NH_3)_5RuOH_2^{3+} \quad (13)$$

could provide an intrinsic equilibration pathway even in the absence of added Ru(II). Decomposition via this pathway is negligible, however, since $K_{11} = 3.5 \times 10^{-8}$ for the μ-isonicotinato and 7×10^{-10} for the μ-isonicotinamido complex above pH 4.3.

For the isonicotinate-bridged complex, R = CO_2^-, formation of the bridged complex is thermodynamically optimized at pH 3–4, above the carboxylic acid pK ~3, and below the aquo pK ~4. The overall binding constant (eq 1 = eq 9 + eq 10) K_1 = ca. 10^4 M^{-1} is comparable to those reported[27] for haloacetate ligands (e.g., $CH_2ICO_2^-$) with pK_a values similar to that of $(NH_3)_5Ru^{II}(4\text{-py}CO_2H)^{2+}$. The thermodynamics of the two catalytic steps can be evaluated from data determined in this study and published[28] values for the $(NH_3)_5RuOH_2^{3+/2+}$ (+0.07 V vs NHE) and $(NH_3)_5RuOH^{2+/+}$ (–0.42 V vs NHE) couples. The substitution reaction eq 9 is pH-independent below ca. pH 11, and from K_1 = ca. 10^4 M^{-1} and the reduction potential for the carboxylate-bound site in the binuclear complex, ~0.05 V vs NHE, the affinity of $(NH_3)_5RuOH_2^{2+}$ for the complexed pyridinecarboxylate, K_9, is ca. 10^2 M^{-1}. The rate constant for eq 9 is expected to be[29-31] 10^{-2} to 10^{-1} M^{-1} s^{-1}, consistent with our qualitative observations. In the pH 3–4 range, the electron-transfer eq 10 is slightly uphill but becomes increasingly unfavorable as the pH increases, as does the overall equilibrium, because of the very high affinity of Ru(III) for hydroxide ion.

For the isonicotinamide analog, R = –C(O)NH^-, K_6 = 6.5 M^{-1}.

$$(NH_3)_5Ru(4\text{-py-}C(O)NH_2)^{2+} + (NH_3)_5RuOH^{2+} \rightleftharpoons (NH_3)_5Ru(4\text{-py-}C(O)NH)Ru(NH_3)_5^{4+} + H_2O \quad (6)$$

From the data give in Scheme I, K_9(R = –C(O)NH_2) = ca. 2 $\times$ 10^{-3} M^{-1} and K_{10}(R = –C(O)NH_2) = ca. 1, but the reactions are driven by the deprotonation of the resulting mixed-valence complex. While this analysis is formally correct, the actual situation is more complicated because of the possibilities of isomers and tautomers (discussed next). Presumably, $(NH_3)_5RuOH_2^{2+}$ binds the amide oxygen initially. At some stage isomerization to the N-bound isomer takes place. Thus K_9 (which reflects the stability of the N-bound isomer) probably does not provide an accurate measure of the driving force for the substitutional step.

Nature of the Amido Complexes. Of necessity, the μ-isonicotinato complexes contains the Ru^{III}–O–C(O)–py moiety. The analogous isonicotinamide-based system is potentially more complicated, however, since amides may coordinate a metal center either through oxygen or nitrogen.[32] Recent studies indicate that the deprotonated amide (RC(O)NH^-) ligand binds preferentially through nitrogen, while protonation favors rearrangement to the oxygen-bonded isomer (eq 14).[16,24] The rates for such linkage isomerizations appear to reflect the tautomeric composition of the complex, with isomerization rates correlating with the proportion of –NH_2C(O)R tautomer, the –NHC(OH)R tautomer being relatively unreactive. Because of the potential confusion introduced by linkage isomerism, we also prepared $(NH_3)_5Ru$(4-pyC(O)NH)$Ru(NH_3)_5^{5+}$ via hydrolysis of the parent nitrile complex $(NH_3)_5Ru$(4-pyCN)$Ru(NH_3)_5^{6+}$, a route expected to give the N-bonded isomer as primary product. The electronic absorption spectrum of the product is consistent with this expectation, the ca. 350-nm band being associated with ligand-to-metal charge transfer (N-to-Ru(III) πd). Were the product O-bonded, LMCT should occur at a significantly shorter wavelength (ca. 290 nm as observed for the isonicotinato-bridged complex). As is found for noncomplexed amides,[32] $(NH_3)_5Ru$(4-pyC(O)NH)Ru$(NH_3)_5^{5+}$ is an extremely weak base, with evidence for its protonation being observed only in ≥2 M triflic acid. (By contrast, its reduced form $(NH_3)_5Ru$(4-pyC(O)NH)$Ru(NH_3)_5^{3+}$ (Scheme I) has a pK of ca. 4.3.) In contrast to a number of N-bonded complexes of the neutral amide ligand, $(NH_3)_5Ru$(isonicotinamide)$Ru(NH_3)_5^{6+}$ is not observed to isomerize (at least on the time scale of 1 h or so). This suggests that the imide tautomer, Ru^{III}NH=C(OH)R, is strongly favored (eq 15). We do not

$$Ru^{III}NH_2C(O)R \rightleftharpoons Ru^{III}NH{=}C(OH)R \qquad K \gg 1 \quad (15)$$

$$R = (4\text{-py}Ru^{III})^{3+}$$

believe we have observed the O-bonded isomer of $(NH_3)_5Ru$(isonicotinamide)$Ru(NH_3)_5^{6+}$ in this study, but it is expected to be substantially less acidic (pK_a ≥9).

One-electron reduction of $(NH_3)_5Ru^{III}(\mu\text{-4-pyC(O)NH})Ru^{III}(NH_3)_5^{5+}$ results in reduction of the ruthenium bound to the pyridine nitrogen. This is evident from the appearance of the intense Ru(II)-to-pyridine MLCT band in the visible region and from the position of the first reduction potential of the diruthenium(III) complex at ca. +0.4 V vs NHE, a value characteristic of this moiety.[28,33] Again, questions of isomerism of the amide ligand arise and again all evidence points to a single isomer, the N-bonded form. First, we obtain the same electronic absorption spectrum for $(NH_3)_5Ru^{II}$(isonicotinamido)$Ru^{III}(NH_3)_5^{4+}$ whether we generate it by rapid ($Ru(NH_3)_6^{2+}$) reduction of $(NH_3)_5Ru^{III}(\mu\text{-4-pyC(O)NH})Ru^{III}(NH_3)_5^{5+}$ or prepare it from $(NH_3)_5Ru$(4-pyC(O)NH_2)$^{2+}$ and $Ru(NH_3)_5OH_2^{3+}$ (followed by chromatography). Were this product the O-bonded isomer, an unprecedentedly rapid ($k_{obs} \geq 0.1$ s^{-1}) N-to-O isomerization rate would be required. Secondly, the ca. 340-nm band in the spectrum of the 4+ species indicates retention of the amide Ru–N bond. In addition, the reduction potential of the amido terminus (–0.15 V vs NHE for the deprotonated isonicotinamide, +0.07 V vs NHE for the neutral ligand; see Scheme I) is characteristic of an N-bound species, for example the benzamide complex[19] and other values in the literature.[16-19]

Reduction Potentials. Both binuclear complexes exhibit two well-separated redox processes. The first reduction (eq 16) at ca. +400 mV vs NHE is that of the pyridine-bonded ruthenium(III).

$$(NH_3)_5Ru^{III}(4\text{-pyR})Ru^{III}(NH_3)_5 + e^- \rightleftharpoons (NH_3)_5Ru^{II}(4\text{-pyR})Ru^{III}(NH_3)_5 \qquad E_{py} \quad (16)$$

The values determined here for that process (Tables I and III) are quite unremarkable. The second reduction is that of the carboxylato- or amido-attached ruthenium(III) (eq 17). This

$$(NH_3)_5Ru^{II}(4\text{-pyR})Ru^{III}(NH_3)_5 + e^- \rightleftharpoons (NH_3)_5Ru^{II}(4\text{-pyR})Ru^{II}(NH_3)_5 \qquad E_R \quad (17)$$

$$(NH_3)_5Ru^{II}(4\text{-pyR})Ru^{II}(NH_3)_5 \rightleftharpoons (NH_3)_5Ru^{II}(4\text{-pyR}) + (NH_3)_5RuOH_2^{2+} \quad (18)$$

process is not chemically reversible, because the ruthenium(II) in these complexes is quite labile[12,14,15] and hydrolyzes (eq 18) (possibly first isomerizing in the case of the amido species[16]). As noted above, the E_R values are similar to those reported for other systems. The reduction potential for the carboxylate site in the binuclear complex, –0.05 V vs NHE, is similar to that for

Table IV. Mixed-Valence $((NH_3)_5Ru)_2(\mu\text{-pyR})$ Complexes[a]

	R = 4-C(O)O–	R = 4-C(O)NH–	R = 4-C≡N–
$E°$, V vs NHE	+0.394, –0.046[a]	+0.392, –0.15	+0.684, +0.409[b]
$\Delta E°$, V	0.44	0.54	0.275
λ_{max}(IT), nm (ϵ, M^{-1} cm^{-1})	720 (295)[a]	761 (9 × 10^2)	935 (1.1 × 10^3)[b]
$\Delta\nu_{1/2}$(IT), cm^{-1}	5060	4620	5170[b]
H_{rp}(IT),[c] cm^{-1}	300	510	535[b]
E_{op}(IT), eV	1.72	1.63	1.33
λ(IT), eV (E_{op} – $\Delta E°$ – 0.25)	1.03	0.84	0.80
r(M–M), Å	9.0	9.0	9.3[b]
λ_{max}(MLCT), nm (ϵ, M^{-1} cm^{-1})	471 (7.0 × 10^3)	450 (0.8 × 10^4) 500 (sh) (6.4 × 10^3)	493 (1.0 × 10^4)[b]
λ_{max}(LMCT), nm (ϵ, M^{-1} cm^{-1})	290 (sh) (3.5 × 10^3)	336 (3.0 × 10^3)	340 (sh) (3.0 × 10^3)[e]
λ_{max}(IL), nm (ϵ, M^{-1} cm^{-1})	260 (5.0 × 10^3)	256 (3.6 × 10^3)	256 (1.4 × 10^4)[e]
			216 (1.2 × 10^4)[e]

[a] Data from this study in 0.1 M KCF_3SO_3 at pH 4.7 (0.02 M total acetate buffer) unless otherwise noted. [b] Richardson, D. E.; Taube, H. *J. Am. Chem. Soc.* **1983**, *105*, 40. [c] From the expression $H_{rp} = (2.05 \times 10^{-2}/r)[\epsilon_{max}\Delta\nu_{1/2}\nu_{max}]^{1/2}$. [d] Matsubara, T.; Ford, P. C. *Inorg. Chem.* **1976**, *15*, 1107. 0.1 M *p*-toluenesulfonic acid/0.1 M potassium *p*-toluenesulfonate medium. [e] In 0.1 KCF_3SO_3 at pH 3; prepared by in situ persulfate oxidation.

$CH_2ICO_2^-$ ($E°$ for $(NH_3)_5Ru(CH_2ICO_2)^{2+/+}$, –0.03 V vs NHE[13]). The benzamido[19] and μ-isonicotinamido values are the same within error, –0.15 V vs NHE, comparable to that cited by Schäffer and Taube[34] and about 100 mV more positive than those reported for chelated species.[16] Values reported recently by Huang et al.[17] are 0 ± 10 mV vs NHE at pH 5, but recent studies[19] of the pH dependence of the potentials show that these do not reflect the limiting values for the amido couples.

As has been noted previously,[35-37] the potentials are very solvent sensitive when ferrocenium/ferrocene is taken as a solvent-independent reference (Table III). As is shown in Table II and Figure 4, the reduction potentials of the binuclear complexes studied here also exhibit a dependence on solvent donor number. For the μ-isonicotinato complex, the sensitivity of the pyridine-attached metal center to donor number (28.5 mV/DN) is somewhat greater than that of the carboxylato-attached center (24 mV/DN) so that ΔE ($=E_{py} - E_{OCO}$) decreases slightly with donor number. Interaction of the ammine hydrogen atoms with the solvent increases with solvent donor number and, since the Ru(III) N–H bonds are more acidic than those of Ru(II), the stabilization of the Ru(III) complex increases with solvent donor number and the Ru(II)/(III) couple becomes more reducing as donor number increases.

Yeh and Taube[30] have addressed the issue of glycine binding in the context of "ruthenating" (preparing $(NH_3)_5Ru$ derivatives of)[38,39] proteins. However, the issue of $(NH_3)_5Ru$ binding to the protein polypeptide backbone has not been considered. The thermodynamics of binding of some metal ions to amides and polypeptides has been characterized,[32] but our estimate for K_6 is the first to bear on this subject with the ruthenium ammine center. Unfortunately, its value is weakened by our ignorance of the corresponding proton affinity of the amido group. It can be bracketed, however, by that of the free ligand, 21.5 in DMSO[40] and 22.1 in DMF[41] at 25 °C. (For benzamide, the analogous values are 23.3 and 23.9.) Using benzoic acid, for which pK_a values in both water and DMSO have been determined, to model the solvent dependence, values of 14.7 and 16.5 are estimated for isonicotinamide and benzamide in water. These are consistent with the estimate of 15.1 proposed earlier.[32] Under the assumption that K_6 and the amido reduction potential are applicable to the polypeptide backbone, at pH 7, these considerations lead to the conclusion that the distribution of $Ru^{II}(NH_3)_5L$ at equilibrium

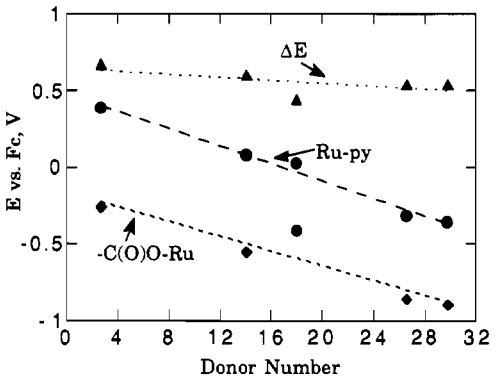

Figure 4. Solvent dependence of the Ru(III)/Ru(II) reduction potentials for the μ-isonicotinato complex.

strongly disfavors the polypeptide backbone (L, effective equilibrium constant per residue at pH 7, M^{-1}): histidine 2 × 10^5, glycine 4 × 10^2, $-C(O)O^-$ 100, –NHC(O)R (polypeptide unit) 2.[13,27,30,42,43] Consistent with experimental observations,[38] the equilibrium distribution of $Ru^{III}(NH_3)_5L$ at pH 7 still favors histidine significantly but then suggests the amido site over other common residues: histidine 2 × 10^3, –NHC(O)R (polypeptide unit) 6, glycine 0.4, $-C(O)O^-$ 0.1. This is an area which merits and should prove tractable to more systematic study.

Spectra. The features of the electronic absorption spectra of the species studied here are summarized in Tables I and IV. Intraligand π-to-π^* absorptions occur in the 200–280-nm region. The position of the LMCT band of the isonicotinate-bridged complex, 290 nm, is characteristic of the Ru^{III}–O–C(O) chromophore.[12,13] The MLCT absorption for the mixed-valence μ-isonicotinato complex (471 nm in water) is intermediate in energy between that of the pyridine-bound mononuclear isonicotinate complex (460 nm) and its conjugate acid (492 nm), consistent with the electron-withdrawing ability of the $Ru^{III}(NH_3)_5$ moiety being less than that of a proton. Interestingly, with $(NH_3)_5Co^{III}$ attached to the carboxyl group, the MLCT maximum is essentially the same (λ_{max} 490 nm)[44] as for the protonated species. As would be expected,[35-37] the Ru(II)-to-pyridine MLCT band shifts to longer wavelength (Table III) as solvent donor number increases, reflecting the increasing donor ability of Ru(II) (Figure 4).

Ruthenium(III) amido complexes exhibit bands in the 320–400-nm regions attributable to ligand-to-metal charge transfer from the nitrogen lone pair of the deprotonated NH_2 group to the half-empty πd orbital of Ru(III).[11,18,19] Surprisingly, the LMCT absorptions in the 4+ and 5+ μ-isonicotinamido complexes

(35) Curtis, J. C.; Sullivan, B. P.; Meyer, T. J. *Inorg. Chem.* **1983**, *22*, 224–236.
(36) Chang, J. P.; Fung, E. Y.; Curtis, J. C. *Inorg. Chem.* **1986**, *25*, 4233–4241.
(37) Creutz, C.; Chou, M. H. *Inorg. Chem.* **1987**, *26*, 2995–3000.
(38) Mathews, C. R.; Erickson, P. M.; Van Vliet, D. L.; Petersheim, M. *J. Am. Chem. Soc.* **1978**, *100*, 2260–2262.
(39) Yocom, K. M.; Shelton, J. B.; Shelton, J. R.; Schroeder, W. A.; Worosila, G.; Isied, S. S.; Bordignon, E.; Gray, H. B. *Proc. Natl. Acad. Sci. U.S.A.* **1982**, *79*, 7052–7055.
(40) Bordwell, F. G. *Acc. Chem. Res.* **1988**, *21*, 456–463.
(41) Maran, F.; Celadon, D.; Severin, M. G.; Vianello, E. *J. Am. Chem. Soc.* **1991**, *113*, 9320–9329.
(42) These orderings are based on a pH 7 solution, pK's for the potential ligand residues of 8.3 ($-NH_2$ in glycine), 6.0 (histidine N), and 4.0 ($-CO_2H$), and binding constants given for the ethyl glycinate ester, imidazole, and carboxylate[13,27] ligands and our own values for the amide.[30,43] The values for Ru(III) also consider the pK of this species.
(43) Kuehn, C. G.; Taube, H. *J. Am. Chem. Soc.* **1976**, *98*, 689–702.
(44) Isied, S. S.; Vassilian, A. *J. Am. Chem. Soc.* **1984**, *106*, 1726–1732.

occur at somewhat higher energy (340 and 350 nm) than is usually found (360–400 nm[11,17]) for the Ru^{III}–NH–C(O) chromophore. This shift cannot be attributed to diminished electron-acceptor ability of the metal center since the reduction potentials of the benzamido and isonicotinamido complexes are the same. Both $(NH_3)_5Ru^{II}$ and $(NH_3)_5Ru^{III}$ substituted on the pyridine nitrogen appear to delocalize the NR_2^- electron pair to a greater extent even than CH_3^+ or H^+ in this position. Of course, this is consistent with a simple electrostatic effect, but if this is the explanation, it is surprising that the effect should be so large over this distance. Especially puzzling (and inconsistent with simple electrostatics) is the fact that this transition lies at higher energy for the mixed-valence 4+ species than in its diruthenium(III) counterpart.

As expected, $(NH_3)_5Ru^{II}(\mu\text{-}4\text{-}pyC(O)NH)Ru^{III}(NH_3)_5^{4+}$ exhibits intense absorption in the visible region, characteristic of the Ru^{II}py chromophore.[8] The band maximum (ca. 455 nm in water, depending upon the medium) is shifted about 0.1 eV to higher energy compared to the parent $(NH_3)_5Ru^{II}(4\text{-}pyC(O)NH_2)$ complex (λ_{max} 478 nm in water) and is similar to that reported for polyproline-bridged Ru^{II}–Co^{III} species.[45] This is in the direction and of the magnitude noted above for the isonicotinate complex. However, the band shape is atypical of the $(NH_3)_5Ru^{II}$py chromophore, being rather asymmetric, skewed to higher intensity on the higher energy side (Figure 2) with the suggestion of a shoulder near 500 nm. In polypyridylruthenium(II) complexes such a band shape arises from a vibronic splitting, but such a feature has not been reported for complexes of the $(NH_3)_5Ru^{II}$py series. The shoulder could also arise because of the presence of a second chromophore or because of a second species.[37,46] A second chromophore could be introduced by the presence of the imine moiety, introducing the possibility of both Ru(II)-to-pyridine π^* and Ru(II)-to-imine π^* charge-transfer transitions. Finally, the two species which could be considered are the cis and trans isomers of the N-bonded amido complex (eq 19). Such isomerism has long been established for uncomplexed

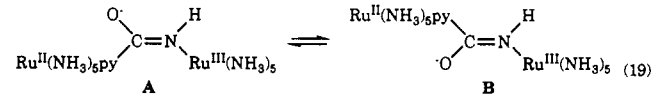

(19)

amides[47] but has not, to our knowledge, been addressed in the coordination chemistry literature. Although the isomerism eq 19 provides a reasonable explanation for the presence of two species, it is not clear why the MLCT bands of the two isomers should differ significantly. Conceivably, a secondary factor, such as preferential hydrogen bonding of one isomer to the $Ru^{III}(NH_3)_5$ ammine hydrogens, is also at work.

Both $(NH_3)_5Ru^{II}(4\text{-}pyC(O)O)Ru^{III}(NH_3)_5$ and $(NH_3)_5Ru^{II}$-$(4\text{-}pyC(O)NH)Ru^{III}(NH_3)_5$ mixed-valence complexes exhibit bands of moderate intensity in the 700–800-nm region, depending on the bridging ligand and the solvent (Tables III and IV). The mixed-metal mixed-valence complex, $(NC)_5Fe^{II}(4\text{-}pyC(O)$-$NH)Ru^{III}(NH_3)_5$, exhibits a similar absorption feature at 645 nm with a molar absorptivity of 5.7×10^2 M^{-1} cm^{-1}.[17] These bands are attributed to intervalence charge transfer or MMCT (metal-to-metal charge transfer) transitions. Focusing on the observations in aqueous media which are summarized in Table IV, the redox free-energy difference ($\Delta E°$) between the pyridine and "saturated" binding sites in the complexes is ca. 0.5 V. From the positions of the MMCT maxima (E_{op}) and $\Delta E°$, λ values ($\lambda = E_{op} - \Delta E° - 0.25$)[25] of 1.03 and 0.84 eV are derived for the isonicotinato and isonicotinamido species, respectively. The values are qualitatively consistent with the band widths at half intensity ($\Delta\nu_{1/2}$). Surprising, however, is the fact that λ for the isonicotinate-bridged species it is so much greater than for the isonicotinamido- or 4-cyanopyridine-bridged species. Conceivably, the extent of charge transfer is greater[37,48,49] for isonicotinate.

The electronic coupling elements H_{rp}, evaluated from the bands' intensities and widths (eq 20), assuming a metal–metal separation (r) of 9 Å, are 300, 510, and 535 (r = 9.3 Å)[5] cm^{-1} for the

$$H_{rp} = (2.05 \times 10^{-2}/r)(\epsilon_{max}\Delta\nu_{1/2}\nu_{max})^{1/2} \quad (20)$$

isonicotinato, isonicotinamido, and cyanopyridine complexes, respectively. For $(NC)_5Fe^{II}(4\text{-}pyC(O)NH)Ru^{III}(NH_3)_5$, a value of 480 cm^{-1} was estimated.[17] Thus significant electronic communication is possible across a $-C(O)O^-$ or $-C(O)NH^-$ moiety, consistent with significant contributions from resonance structures such as

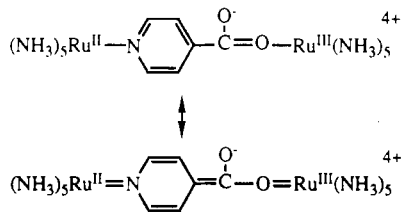

Interestingly, the coupling elements observed for the asymmetric systems are as great as and even greater than those for the symmetric 4,4′-bipyridine (H_{rp} = 390 cm^{-1})[50] and 1,4-dicyanobenzene (H_{rp} = 314 cm^{-1})[5] systems. Of course the distances are greater in the latter. An additional factor which may enhance the MMCT band intensity is the greater mixing of the MMCT state with the MLCT state in certain cases. For example, for the isonicotinato-bridged dimer, the MMCT and MLCT states are separated by 0.91 eV, in contrast to ca. 1.2 eV for the above mentioned symmetric dimers. This factor is discussed in greater detail in the next section. H_{rp} is larger for isonicotinamido than for isonicotinato. If the coupling mechanism involves only the ligand π^* system, this is a surprising result since MLCT occurs at higher energy in the isonicotinamide complex than in the carboxylate-substituted species. This is probably a result of the short Ru–N distance[19] and significant π-N-to-Ru(III) donation.

The isonicotinamido and isonicotinato species prepared here provide potential models for the electronic properties of the N and O termini of a polyproline bridge, respectively. For $n > 0$, the pyridyl group attached to the electron donor is attached to the polyproline bridge through a 4-C(O)N rather than a 4-C(O)O group. The results for the isonicotinamido complex suggest that this moiety differs somewhat from isonicotinate in its electronic characteristics, with the optical H_{rp} (510 cm^{-1}) being greater than that for isonicotinate (300 cm^{-1}). However, the N-protonated isonicotinamide-bridged species, which we have not characterized, would serve as a better point of comparison.

Electronic Coupling Pathways. In addition to the approach used above, the magnitude of the electronic coupling between donor and acceptor sites in covalently attached donor–acceptor complexes may be probed through studies of thermal electron transfer. For the thermal process, the electronic coupling may be evaluated from the limiting rate of the (nonadiabatic, eq 21) reaction in the

$$k = (H_{rp}^2/h)(\pi/\lambda RT)^{1/2}\exp(-\Delta G^*/RT) \quad (21)$$

barrierless regime ($\Delta G^* = 0$) or from the temperature dependence of the rate constant of the (nonadiabatic) donor-to-acceptor electron-transfer reaction (eqs 22–24).[2,51]

$$H_{rp}\ (cm^{-1}) = [\nu_{el}\ (s^{-1})\ \lambda\ (cm^{-1})^{1/2}]^{1/2}/1.52 \times 10^5 \quad (22)$$

$$\nu_{el} = k/\exp(-\Delta H^*/RT) \quad (23)$$

$$\lambda = 4(\Delta H^* - \Delta H°/2) \quad (24)$$

(45) Isied, S. S.; Vassilian, A. *J. Am. Chem. Soc.* **1984**, *106*, 1732–1736.
(46) We reject the possibility that the long-wavelength component is due to a nonbonding d to π^* transition, since the latter transition is much weaker and only observed with extremely π-accepting ligands.[37]
(47) Gutowsky, H. S.; Holm, C. H. *J. Chem. Phys.* **1956**, *25*, 1228–1234.
(48) Oh, D. H.; Boxer, S. G. *J. Am. Chem. Soc.* **1990**, *112*, 8161–8162.
(49) Oh, D. H.; Sano, M.; Boxer, S. G. *J. Am. Chem. Soc.* **1991**, *113*, 6880–6890.
(50) Sutton, J. E.; Taube, H. *Inorg. Chem.* **1981**, *20*, 3125–3124.
(51) Sutin, N. In *Electron Transfer in Inorganic, Organic and Biological Systems*; Bolton, J. R., Mataga, N., McLendon, G., Eds.; Advances in Chemistry Series 228; American Chemical Society: Washington, DC, 1991; pp 25–43.

Table V. Electronic Coupling Parameters for $M^{II}iso(Pro)_nM^{III}$ Systems

n	$k(298)$, s^{-1}	ΔH^*, kcal/mol	ΔS^*, cal/(mol K)	$\Delta E^\circ = \Delta G^\circ$, eV	λ,[a] eV	ν_{el},[b] s^{-1}	H_{rp},[c] cm^{-1}
			Os–Ru[d]				
0	$>5 \times 10^9$	(4.2)[g]		−0.20	(1.12)[g]	$(>10^{13})$[g]	(≥300)[h]
1	3.1×10^6	4.2	−15	−0.25	1.22	3.8×10^9	4.0
2	3.7×10^4	5.9	−19	0.26	1.55	8.1×10^8	2.0
3	3.2×10^2	7.4	−23	−0.26	1.81	8.9×10^7	0.68
			Os–Co[e]				
0	1.9×10^5	10.2	0	−0.29	2.35	5×10^{12}	174
1	2.7×10^2	11.7	−8	−0.33	2.69	9×10^{10}	24
2	7.4×10^{-1}	12.7	−16	−0.33	2.87	1×10^9	2.9
			Ru–Co[f]				
0	1.2×10^{-2}	19.7	−1	+0.37	2.68	4×10^{12}	153
1	1×10^{-4}	18.0	−16	+0.37	2.38	2×10^9	3.2
2	0.6×10^{-5}	18.6	−20	+0.37	2.49	2×10^8	1.3

[a] $\lambda = 4(\Delta H^* - \Delta H^\circ/2)$; ΔH° is assumed equal to ΔG°. [b] $\nu_{el} = k/\exp(-\Delta H^*/RT)$. [c] H_{rp} $(cm^{-1}) = [\nu_{el}\ (s^{-1})\ \lambda\ (cm^{-1})^{1/2}]^{1/2}/1.52 \times 10^5$. [d] Kinetic data and reduction potentials from: Vassilian, A.; Wishart, J. F.; van Hemelryck, B.; Schwarz, H.; Isied, S. S. *J. Am. Chem. Soc.* **1990**, *112*, 7278–7286. [e] Kinetic data and Ru(III) reduction potential from: Isied, S. S.; Vassilian, A.; Magnuson, R. H.; Schwarz, H. A. *J. Am. Chem. Soc.* **1985**, *107*, 7432–7438. The Co(III) reduction potential is taken as +0.06 V vs NHE. [f] Kinetic data and Ru(III) reduction potential from: Isied, S. S.; Vassilian, A. *J. Am. Chem. Soc.* **1984**, *106*, 1732–1736. The Co(III) reduction potential is taken as +0.06 V vs NHE. [g] Obtained by assuming that $k = 5 \times 10^9\ s^{-1}$, $\kappa_{el} = 1$, and $\nu_n = 6 \times 10^{12}\ s^{-1}$ and neglecting any barrier lowering by H_{rp}. [h] Lower limit, based on the value obtained for the diruthenium analog (Table IV).

Isied and colleagues have extensively studied thermal M_1 to M_2 electron-transfer rates for isonicotinylpolyproline-bridged systems.

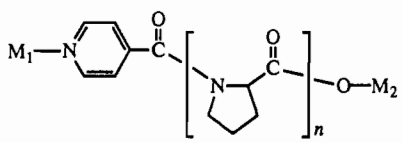

For the $n = 0$, Os^{II}–Ru^{III} derivative, a lower limit of $5 \times 10^9\ s^{-1}$ was reported and it was proposed that electron transfer is adiabatic for this system, with the degree of electronic coupling being possibly so great that barrier lowering is also significant.[6] One objective of this study was the characterization of $(NH_3)_5Ru^{II}$-(4-pyC(O)O)$Ru^{III}(NH_3)_5^{4+}$ as a model for $(NH_3)_5Os^{II}$(4-pyC-(O)O)$Ru^{III}(NH_3)_5^{4+}$, with is $n = 0$ of the polyproline series. To facilitate discussion of the two molecules, their ground- and excited-state energetics are compared in Figure 5. (For Ru(II)–Ru(III), the state positions are based on the values in Table IV. For Os(II)–Ru(III), the MLCT states are modeled by Os-$(NH_3)_4$Cl(isonicotinate)$^+$,[52] ΔG^* is obtained by assuming an adiabatic reaction with $\nu_n = 6 \times 10^{12}\ s^{-1}$, $k = 5 \times 10^9\ s^{-1}$, and $\Delta G^\circ = -0.2$ eV,[6] and the MMCT states are modeled from the values given in the first row of Table V and a spin–orbit correction of 0.37 eV.) For both binuclear complexes, the lowest energy excited states (apart from the MMCT states) are MLCT in nature. LMCT states lie much higher (3.1 eV for pyridine-to-Os(III) LMCT, 4.3 eV for carboxylate-to-Ru(III) LMCT). The MLCT interaction profoundly affects the properties of the complexes in their ground states, being responsible for their colors and the magnitudes of their redox potentials. With Ru(II), the donor site is metal centered, with modest mixing of the aromatic π^* system: The ground-state wave function is estimated[53] to have electron densities (squared wave-function coefficients) of 0.90 and 0.10 for Ru(II) and the isonicotinate ligand, respectively. For the Os(II) case, the metal and ligand orbitals are more extensively mixed,[52-54] with the ground-state wave function estimated to have electron densities of 0.66 and 0.34 on Os(II) and the isonicotinate ligand, respectively. The M(II)–isonicotinate interaction provides a mechanism for the M(II)–M(III) coupling. In terms of first-order perturbation theory, the optical electronic coupling arises through interaction of the MMCT state with the MLCT state. For Ru(II)–Ru(III), the (nonbonding) MLCT and MMCT transitions are separated by 0.6 eV, while for Os(II)–Ru(III), they are nearly in resonance. Thus for Os(II)–Ru(III), H_{rp} for the *optical* electron transfer is expected to be significantly greater than the 300 cm^{-1} estimated here for Ru(II)–Ru(III).

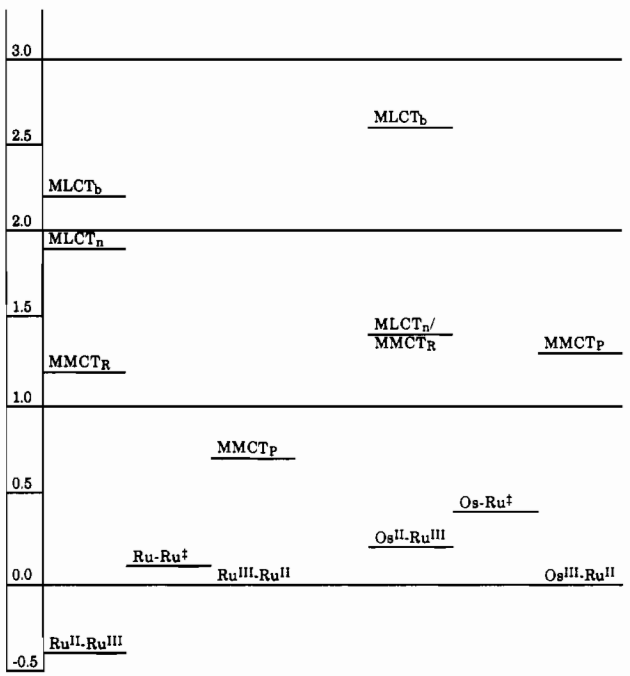

Figure 5. Energetics (electronvolts) of excited-state manifolds of isonicotinato-bridged Ru(II)–Ru(III) and Os(II)–Ru(III) species. The subscripts denote bonding (b), nonbonding (n), reactant (R), and product (P).

The effective electronic coupling element for optical electron transfer is not necessarily equal to that for thermal electron transfer. In general, H_{rp} will differ for optical and thermal electron transfer to the extent that the electronic wave functions of the reactant and product states depend upon their nuclear configurations.[51] In addition, when mixing of donor and acceptor states is dominated by interaction with excited states of the system ("superexchange"), the coupling elements for optical and thermal electron transfer will differ because of the differing energy dif-

(52) Magnuson, R. H.; Taube, H. *J. Am. Chem. Soc.* **1975**, *97*, 5129–5136.
(53) For the Ru(II)–isonicotinate moiety, we have used values given[37,74] for pyrazine as ligand, since Ru(II)–pyrazine and Ru^{II}-4-pyC(O)ORu^{III} complexes have the same MLCT maxima. For the Os(II)–isonicotinate moiety, we have used the analysis of Magnuson and Taube[52] for $(NH_3)_4ClOs^{II}$(4-pyC(O)OH) which has the same principal MLCT maximum (523 nm) as reported[54] for the Co(III)-substituted carboxylate.
(54) Isied, S. S.; Vassilian, A.; Magnuson, R. H.; Schwarz, H. A. *J. Am. Chem. Soc.* **1985**, *107*, 7432–7438.

ferences for the two processes. For simplicity, we consider interaction with a single MLCT excited state of the system. For optical electron transfer, the relevant energy differences are $\Delta E_{r/B}(Q_r°)$ and $\Delta E_{p/B}(Q_r°)$, the differences between the energies of the MLCT state and the energies of the reactant and product states, respectively, at the equilibrium nuclear configuration of the reactants ($Q_r°$). These are

$$\Delta E_{r/B}(Q_r°) = E_{MLCT} \quad (25a)$$

$$\Delta E_{p/B}(Q_r°) = E_{MLCT} - (\lambda_{DA} + \Delta G°) \quad (25b)$$

where λ_{DA} is the reorganization parameter and $\Delta G°$ is the free-energy change for the donor–acceptor electron transfer. The energy gap determining the electronic coupling element for the optical electron transfer is[55]

$$\Delta E_{op} = [2\Delta E_{r/B}(Q_r°)\Delta E_{p/B}(Q_r°)]/[E_{r/B}(Q_r°) + \Delta E_{p/B}(Q_r°)] \quad (25c)$$

For thermal electron transfer, the electronic coupling arises through interaction of the transition state with the MLCT state. The difference between the energy of the MLCT state and that of the reactants at the transition-state configuration is[51,56]

$$\Delta E_{th} = \Delta E_{rp/B}(Q_r^*) = \Delta E_{MLCT} - \lambda_D(1 + \Delta G°/\lambda_{DA}) \quad (26)$$

where λ_D is the reorganization parameter for the D,D^+ couple. Since the effective electronic coupling elements in the superexchange mechanism are proportional to the reciprocals of the relevant energy gaps, it follows that

$$H_{rp}^{th}/H_{rp}^{op} = 1 - [E_{MMCT}/(2E_{MLCT} - E_{MMCT})]^2 \quad (27)$$

where $E_{MMCT} = \lambda_{DA} + \Delta G°$ and it has been assumed that $\lambda_D = \lambda_{DA}/2$. Within this model, the coupling element for optical electron transfer is never less than that for thermal electron transfer; however, in typical systems the two are likely to differ by less than 25%. For Ru(II)–Ru(III), $\Delta E_{rp/B}$ is estimated to be 1.7 eV, while for Os(II)–Ru(III) it is about 0.7 eV. On this basis, we propose that H_{rp}^{op} for Ru–Ru may provide a reasonable estimate for the lower limit of H_{rp}^{th} for Os(II)–Ru(III). A value of 300 cm^{-1} for H_{rp}^{th} for Os(II)–Ru(III) is certainly not inconsistent with the estimates extracted for this system and given in Table V. Such a value leads to fully adiabatic electron transfer in this system and, when λ is taken as 1.1 eV and $\Delta G°$ as −0.2 eV, $\Delta G^* = 0.20$ eV is calculated (observed $\Delta G^* \leq 0.18$ eV), consistent with the modest barrier lowering of 300 cm^{-1} (0.037 eV).

Polyproline-Bridged Systems. We turn next to the electronic coupling parameters for polyproline-bridged systems. H_{rp} values obtained from analysis of the experimental data[6,45,54] according to eqs 21–24 are given in Table V. (Those for Ru–Co are included for the sake of completeness but will not be discussed further because the rates are so slow that they probably reflect the reactivities of several conformers. The other data sets have been truncated to include only the more rapid systems for the same reason.) In Figure 6, H_{rp} values from Table V and the literature[51] are plotted as a function of the number of bridging atoms for polyenes,[48,49] polymethylene,[50,57] and polyproline[6,54] residues. The slopes vary over a considerable range. For the polyproline bridge, the slope for Ru(III) on the carboxyl terminus is 40% smaller than with Co(III) on the carboxyl terminus, in contrast to a conclusion drawn in earlier work.[6,58] However, there is a conceptual problem in comparing the $n = 0$ derivative with the other members of the series since their excited-state energetics differ so profoundly. MLCT and LMCT states of the polyproline must be critical to the electronic coupling in the $n > 0$ species, but the metal centers in the $n = 0$ species should derive significant electronic communication through the much lower energy MLCT states of the

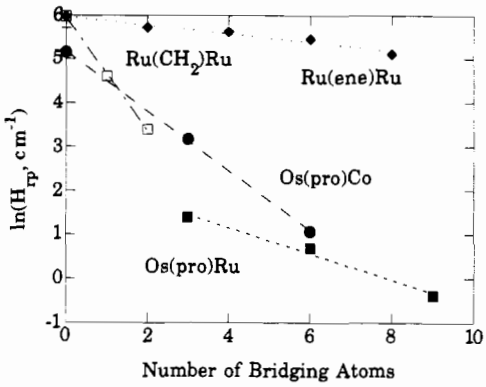

Figure 6. Natural logarithm of the reactant–product electronic coupling element inferred for polyene ($\alpha_b = 0.9$) and polymethylene Ru(II)–Ru(III), and polyproline Os(II)–Co(III) ($\alpha_b = 0.54$) and Os(II)–Ru(III) ($\alpha_b = 0.74$) spaced donor–acceptor pairs as a function of the number of bonding atoms separating the donor and acceptor.

pyridyl ligand. Thus the discontinuity observed between $n = 0$ and 1 of the Os(II)–Ru(III) data in Table V is consistent with involvement of the pyridyl MLCT states for $n = 0$, in striking contrast to the monotonic dependence on distance observed for the Os(II)–Co(III) data and in the polyene data.

With the introduction of proline units to separate the donor and acceptor sites, the energies of the states of the polyproline bridge must be addressed.[59] At this time, it is difficult to address the energetics of the bridge states in a rigorously quantitative way. While a number of small peptide complexes have been characterized, and in some cases LMCT transitions have been assigned, the positions of MLCT transitions must be entirely inferential at this point. A very rough gauge of the oxidizability and reducibility of polypeptides in general may be gleaned from the solvent limits of DMF, +1.4 and −2.9 V vs NHE, respectively. In agreement with the former, tertiary amides are oxidized at about +1.35 V vs SCE in acetonitrile.[60] Peptides and simple amides exhibit no intense electronic absorptions above 220 nm; for *N*-methylacetamide the $n\rightarrow\pi^*$ transition lies at 210 nm, and the $\pi\rightarrow\pi^*$ transition lies at 188 nm.[61]

In terms of the superexchange description of long-range electronic coupling between the donor and acceptor separated by n (identical) bridging (B) units[62–66]

$$H_{rp} = (H_{DB}H_{BA}/\Delta E_{rp/B})(H_{BB}/\Delta E_{rp/B})^{n-1} \quad (28)$$

where H_{DB} is the coupling element between the donor terminus and the relevant bridge state, H_{BA} is the coupling element between the relevant bridge state and the acceptor, H_{BB} is the coupling element between adjacent bridge units, and as before, $\Delta E_{rp/B}$ is the (vertical) energy separation between the transition state and the relevant bridge state. Since, in general, both "electron" and "hole" conduction pathways may be operative, the relevant states are B^- and B^+ and eq 28 may be rewritten

$$H^-_{rp} = (H^-_{DB}H^-_{BA}/\Delta E^-_{rp/B})(H^-_{BB}/\Delta E^-_{rp/B})^{n-1} \quad (29a)$$

$$H^+_{rp} = (H^+_{DB}H^+_{BA}/\Delta E^+_{rp/B})(H^+_{BB}/\Delta E^+_{rp/B})^{n-1} \quad (29b)$$

When several coupling mechanisms operate in a particular system, their contributions may interact in a complicated way.[66] For the

(55) Newton, M. D. *Chem. Rev.* **1991**, *91*, 767–792.
(56) Siddarth, P.; Marcus, R. A. *J. Phys. Chem.*, in press.
(57) Fischer, H.; Tom, G. M.; Taube, H. *J. Am. Chem. Soc.* **1976**, *98*, 5512–5517.
(58) Endicott, J. F. *Acc. Chem. Res.* **1988**, *21*, 59–66.
(59) Isied, S. S. *Prog. Inorg. Chem.* **1984**, *32*, 443–517.
(60) O'Donnell, J. F.; Mann, C. K. *J. Electroanal. Chem. Interfacial Electrochem.* **1967**, *13*, 163–166.
(61) Li, Y.; Garrell, L.; Houk, K. N. *J. Am. Chem. Soc.* **1991**, *113*, 5895–5896.
(62) McConnell, H. M. *J. Chem. Phys.* **1961**, *35*, 508–515.
(63) Larsson, S. *J. Am. Chem. Soc.* **1981**, *103*, 4034–4040.
(64) Larsson, S. *J. Chem. Soc., Faraday Trans. 2* **1983**, *79*, 1375–1388.
(65) Larsson, S. *Chem. Scripta* **1988**, *28A*, 15–20.
(66) Broo, A.; Larsson, S. *Chem. Phys.* **1990**, *148*, 103–115.

case of a single bridging unit their contributions are simply summed, but "mixing" leading to interference effects may occur with several bridging units.

Of particular interest are the distance dependences observed for the Os(II)–Co(III) and Os(II)–Ru(III) systems in Table V and Figure 6. From the intercepts in Figure 6, $H_{DB}H_{BA}$ is greater for Co(III) (174 cm^{-1}) than for Ru(III) (10 cm^{-1}) as electron acceptor, requiring if H_{DB} is constant, that H_{BA} be 1 order of magnitude greater for Co than for Ru. By contrast, from the slopes, $H_{BB}/\Delta E_{rp/B}$ (per bond) is smaller for Os(II)–Co(III) (0.52) than for Os(II)–Ru(III) (0.74), requiring if H_{BB} is constant, that $\Delta E_{rp/B}$ be about 40% greater for Co than for Ru. If a common coupling mechanism is operative, this pattern strongly suggests that it is a "hole" transfer mechanism; Co(III), with a σ-symmetry acceptor orbital, is expected to have significantly greater overlap with the filled σ-states of the bridge (large H^{+}_{BA}). By contrast, Ru(III), with its π-acceptor orbital, should interact more effectively with filled and empty π levels of the bridge. The relatively large intercept for Os(II)–Co(III) then suggests the operation of a σ-hole mechanism.

We next consider whether the energetics of the two systems are consistent with a hole-transfer pathway. The LMCT transitions of the complexes provide information about the relative energetics of the $B^{+}A^{-}$ states. The LMCT states of both Co(III)[67,68] and Ru(III)[69] pentaammines have been spectroscopically characterized.[70] The lowest energy transition involves transfer of a nonbonding p_x, p_y X^{-} electron. (For Co(III),[67,68] and presumably for Ru(III) as well, transitions involving promotion of the σ-bonded carboxylate oxygen bound to the metal lie at ca. 1 eV higher energy.) For Co(III) the acceptor orbital has been assigned as d_{z^2}, and the LMCT thus results in formation of low-spin Co(II).[67] For low-spin d^5 Ru(III) or Os(III), the π-X^{-}-to-t_{2g} (d_{xz}, d_{yz}) transition is observed.[69] For the π-carboxylate-to-metal LMCT, the LMCT states lie at 5.2 eV (Co(III)) and 4.3 eV (Ru(III)) above the reactants. LMCT from the amide N lone pair occurs at lower energy, for Ru(III) at ca. 3.2 eV (acetamide); on the basis of the electrochemical solvent limit of *N,N*-dimethylformamide, ca. +1.4 V vs NHE, and an estimated carboxylate redox potential of 2.1 V vs NHE,[71] the $B^{+}A^{-}$ LMCT states lie at 4.7 eV (low-spin Co(II)) and 3.6 eV (Ru) above the reactant states, and 3.8 and 3.1 eV above the Os(II)–Co(III)[72,73] and Os(II)–Ru(III) transition states (eq 25), respectively. These considerations lead to the conclusion that, for hole transfer, $H^{+}_{BA}(Co) \gg H^{+}_{BA}(Ru)$, and that $\Delta E^{+}_{rp/B}$ is about 20% greater for Co than for Ru, in qualitative agreement with the experimental distance dependences, which require $\Delta E_{rp/B}(Co) = 1.4\Delta E_{rp/B}(Ru)$.

By contrast, if a single mechanism involving "electron" transfer is operative, since the donor is common and the transition-state positions are very similar in energy, H^{-}_{DB}, H^{-}_{BB}, and $\Delta E^{-}_{rp/B}$ should be about the same for the two acceptors. From the other electrochemical solvent limit for DMF (−2.9 V vs NHE), the Os(III)/(II) reduction potential (−0.3 V vs NHE), and an assumed λ_D value for the transition of 1.5 eV, the $D^{+}B^{-}$ states should lie 4.1 eV above the reactant states or 3.6 eV above the Co and Ru transition states. As noted earlier, $H^{-}_{BA}(Co)$ is expected to be much smaller than $H^{-}_{BA}(Ru)$. Thus, for an electron-transfer pathway, Os–Co and Os–Ru should exhibit similar distance dependences, but the (extrapolated) $n = 0$ intercept should be greater for Ru than for Co as acceptor. In summary, the observed distance dependences for the polyproline-bridged systems appear inconsistent with an exclusively electron-transfer pathway and consistent with a hole-transfer pathway for both systems, although a mixture of hole and electron pathways for the Ru acceptor cannot be ruled out.

Concluding Remarks. Both carboxylato and amido ligands have sufficient affinity for pentaammineruthenium(III) that binuclear complexes bridged by isonicotinato and isonicotinamido ligands can be assembled. The amido complexes are N-bonded to the amide function (as well as to the pyridine nitrogen). The differential stabilization of Ru(III) over Ru(II) is greater for the amido than the carboxylato ligand. Pentaammineruthenium(III) serves as an electron-withdrawing group (but inferior to the proton), as determined from the positions of the Ru(II)–pyridine MLCT band energies. Both bridges provide significant coupling between Ru(II) and Ru(III) metal centers in the mixed-valence complexes. These coupling energies serve as a point of departure for a consideration of coupling mechanisms in related bridged systems for which thermal electron-transfer rates have been determined. It is concluded that hole-transfer pathways predominate when osmium(II) pentaammine is the donor and cobalt(III) or ruthenium(III) pentaammine is the electron acceptor.

Acknowledgment. This research was carried out at Brookhaven National Laboratory under Contract DE-AC02-76CH00016 with the U.S. Department of Energy and supported by its Division of Chemical Sciences, Office of Basic Energy Sciences. We thank Dr. B. S. Brunschwig for his assistance with some of the experiments.

(67) Miskowski, V. M.; Gray, H. B. *Inorg. Chem.* **1975**, *14*, 401–405.
(68) Jorgensen, C. K. *Adv. Chem. Phys.* **1963**, V, 33–146.
(69) Verdonck, E.; Vanquickenborne, L. G. *Inorg. Chem.* **1974**, *13*, 762–764.
(70) Lever, A. B. P. *Inorganic Electronic Spectroscopy*, 2nd ed.; Elsevier: New York, 1984.
(71) Billing, R.; Zakharova, G. V.; Atabekyan, L. S.; Hennig, H. *J. Photochem. Photobiol. A: Chem.* **1991**, *59*, 163–174.
(72) For low-spin Co(II) an excited-state energy of 0.9 eV and λ_A of 1 eV have been used.[73]
(73) Newton, M. D. *J. Phys. Chem.* **1991**, *95*, 30–38.
(74) Zwickel, A. M.; Creutz, C. *Inorg. Chem.* **1971**, *10*, 2395–2399.